

# Nickel and Cobalt Metal-organic frameworks as advanced electrode materials for electrochemical energy storage and ion sensor application

[<sup>1</sup>] Krishnamurthy G, [<sup>2</sup>] Omkaramurthy B M, [<sup>3</sup>] Sangeetha S

[<sup>1</sup>][<sup>2</sup>][<sup>3</sup>] Department of Studies in Chemistry, Bangalore University, Central College Campus, Bangalore-560 001.

**Abstract:** - The metal-organic frameworks are the crystalline porous materials of great importance in the fields of energy and environment due to their high surface area and controllable porous structure. In this paper, we present a new solvothermal approach for the synthesis of Ni and Co based MOFs, which exhibit high electrochemical performance. The electrodes of the above Ni-MOF and Co-MOF have been tested for super capacitor and sensor application. The maximum specific capacitance of Ni-MOF was found to be 202F g<sup>-1</sup> at a scan rate of 1 A g<sup>-1</sup> (about 99% capacitance retention after 2000 cycles), which corresponds to a very high energy density of 36.36 W h kg<sup>-1</sup> and power density of 0.037 W kg<sup>-1</sup>. The Co-MOF electrode was used to find the electron transfer capability, which in turn to detect thiocyanate ions. An excellent sensing property and cycling stability were observed with Co-MOF electrode. The Ni-MOF and Co-MOF would be the most promising electrode materials for the hybrid super capacitor and sensor application as studied using the three-electrode system in 0.6 M KOH solution.

**Index Terms:** Ni-MOF, Co-MOF, thiocyanate, super capacitor, charge/discharge, sensor.

## 1. INTRODUCTION

MOFs represent a new class of nanoporous crystalline solids which consist of metal ions/clusters and multifunctional organic linkages that generate an excess of crystals with three dimensional (3D) structures during self-assembly at a molecular level. [1-2] The organic linkers are generally multidentate organic ligands such as carboxylate, azoles or nitrites. MOFs have attracted great research importance due to their extraordinary properties such as fascinating architecture and topology, tuneable pore size, and exceptionally large surface area. [3-4] Because of the remarkable properties and facile synthesis, MOFs have been widely applied for different applications, such as gas storage, sensors, separation, catalysis, magnetism and drug delivery. [5-8] On the other hand, the redox behaviour of metal cations inside MOFs also enables them to be considered for energy storage application especially as a pseudo capacitive material for super capacitors. [9-10] However, the research focused on potential uses of MOFs as an electrode for super capacitors is in its infancy. Electrochemical capacitors (ECs), also known as super capacitors (SCs), have attracted a great deal of attention because of their supernormal power density, great reversibility, long cycle life, and excellent intrinsic safety. [11-14] Among these SCs, hybrid super capacitors are considered to be hopeful candidates for electrochemical energy storage devices, and they are usually composed of a battery-type (faradaic) electrode material as the source of energy and a capacitor-type (non-faradaic) electrode material as the origin of power. [15-19] Therefore, hybrid super capacitors could hold promise to realize battery-level energy

density together with high power density as super capacitors. [20-22] In this work, we report for the solvothermal method to synthesize Ni-MOF investigated their electrochemical performance as electrode material for SCs. The unique Ni-MOF showed higher specific capacitance and better cycling stability and rate capability. It is believed that the Ni-MOF could serve as a shows potential candidate for super capacitor materials because of their high capacity and low cost as well as environmental friendliness.

Also, we have focused on synthesis conditions and the morphologies of the Ni-MOF and Co-MOF. These MOF shave been formed by heating a mixture of organic linker such as Terephthalic acid and 18-crownether with metal ion in a solvent system that usually contains *N,N*-dimethylformamide functional group. These MOFs or macromolecules are linked through hydrogen bonding and the electrochemical behaviour towardsthiocyanate ion has been studied and super capacitor application.

## 2. EXPERIMENTAL

### 2.1 Materials and Apparatus

Ni (NO<sub>3</sub>)<sub>2</sub>.6H<sub>2</sub>O, Co (NO<sub>3</sub>)<sub>2</sub>.6H<sub>2</sub>O, Terephthalic acid, Methyl imidazole, 18-crownether and DMF were purchased from Merck Chemicals. These were analytical grades chemicals used without further purification. Cyclic voltammetry (CV), galvanostatic charge/discharge (GCD) and electrochemical impedance spectroscopy (EIS) measurements were carried out using a CHI660D electrochemical workstation (Shanghai Chen Hua, Inc.). A conventional three-electrode cell was used and it was equipped with a Pt foil as the counter

electrode and a saturated calomel electrode (SCE) electrode as the reference electrode. All experiments were carried out at room temperature and in 6 M KOH solution.

### 2.2 Synthesis procedure

**Ni-MOF:** Ni (NO<sub>3</sub>)<sub>2</sub>·6H<sub>2</sub>O (1.0 gm), Terephthalic acid (0.70 gm) and were dissolved separately in 25 ml of DMF with mild stirring and then added about 0.5 ml of 1-methylimidazole to get a clear solution. Obtained solution was heated at 120°C for 72 h in a 60 ml Teflon-lined stainless steel autoclave in an hot air oven and then cooled at 5°C to room temperature. The obtained crystals were washed with fresh DMF and chloroform to remove the unreacted substances and finally dried at room temperature.

**Co-MOF:** 18-crownether (0.0204 g.) and Co (NO<sub>3</sub>)<sub>2</sub>·6H<sub>2</sub>O (0.0297 g.) dissolved in DMF solvent (30 mL) separately and the solution was transferred into a 60 ml Teflon-lined stainless steel autoclave and heated at 120°C for 72 h. The autoclave was cooled at 5°C to room temperature. The obtained crystals were washed with DMF and chloroform solvents to remove the unreacted substances and impurities. The product was dried at room temperature.



**Fig 1. Schematic representation of formation of Ni and Co-MOFs.**

### 2.3 Characterization Techniques

The above product was characterized by studying the Powder X-ray diffraction (PXRD) analysis to obtain the information on the purity, phase structure and nature (crystalline or amorphous) of the product. The vibrational properties of the functional groups on Shimadzu 8400S FTIR spectrophotometer using KBr pellets. FE-SEM images were taken on the Zeiss field emission scanning electron microscope. The electrochemical experiments were carried out using an Auto lab PGSTAT30 model Instrument with pilot integration controlled by GPES 4.9 software in a three-compartment cell.

## 3. RESULTS AND DISCUSSION

### 3.1 FT-IR spectral analysis:

FT-IR spectrum (Fig 2a) of Ni-MOF has absorption band in the region 3116cm<sup>-1</sup> which could be due to aromatic C-H stretching vibration originating from the Terephthalic acid.

The weak and strong bands at 1555 and 1330 cm<sup>-1</sup> respectively are assigned as carbonyl C=O of the Terephthalic acid and C-C skeletal vibration of the aromatic ring. The strong band centred at 1106 cm<sup>-1</sup> corresponds to the C-O stretching vibration. The bands at 528 to 668 cm<sup>-1</sup> are assigned as ring in-and-out-of-plane bending vibrations of the aromatic ring.

The IR spectrum of Co-MOF (Fig2b) has shown wide absorption band in the region 3200–3400cm<sup>-1</sup> for O-H stretching vibration of the water molecules. The C-O-C peak was observed at 1345 cm<sup>-1</sup> and the bands at about 1632 and 1390 cm<sup>-1</sup> implied us the presence of NO<sub>2</sub> group.

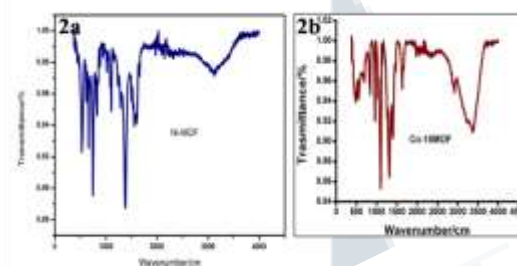


**Fig.2a and 2b: FTIR spectra for Ni-MOF and Co-MOF respectively.**

### 3.2 P-XRD analysis

Powder XRD pattern (Fig.3) for the product was obtained by employing the monochromatic high-intensity CuKα radiation (λ= 0.1541874 nm). The sharpness of the peaks in the pattern indicates the crystalline nature of the product. The prominent metallic peaks of Ni-MOF and Co-MOF are corresponding to the 2θ values, 10.6 and 12.5, 13.0 and 15.27, 29.09, which indicate the coordination of metal with the ligands to form complex. The pattern without much of noise and extra peaks hint us about the purity and pure phase structure of the products obtained. The theoretical (simulated) PXRD pattern calculated from the single-crystal XRD data is in good agreement with the experimental pattern, which confirms that the product is highly crystalline and phase-pure.

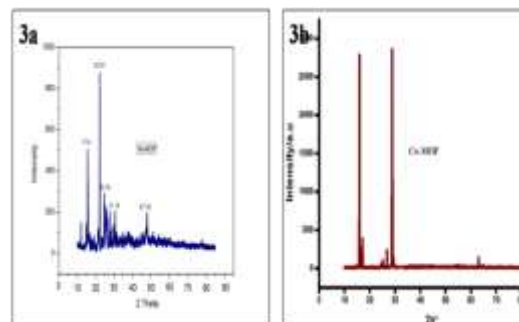


**Fig. 3a and 3b: PXRD patterns for Ni-MOF and Co-MOF respectively.**

### 3.3 FE-SEM analysis

FE-SEM image of Ni-MOF is presented in Fig. 4a shows the Scanning electron microscopy images. The SEM is a technique that enables the study of the microstructure and surface morphology of the products. The SEM micrographs show the distribution of particles of Ni-MOF in a range of dimensions as sheets or layers like structures. The FE-SEM images were viewed at 2 $\mu$ m and 20 $\mu$ m magnifications.

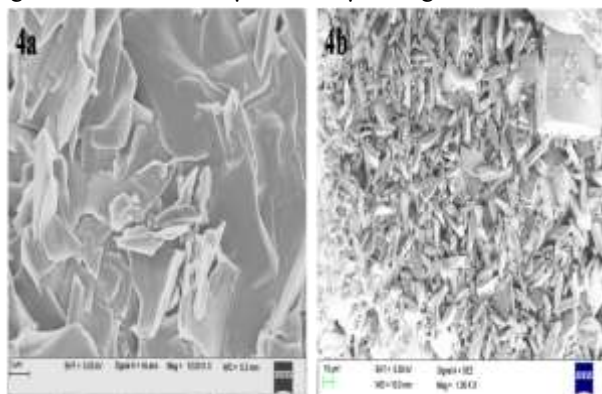


Fig.4a and 4b: FE-SEM images of Ni -MOF and Co-MOF different magnifications (2 and 10 $\mu$ m) respectively.

The flakes like structures of Co-MOF (Fig 4b) were observed under FE-SEM microscope. The particle size was in a range of 1- 4 $\mu$ m.

## 4. ELECTROCHEMICAL STUDIES

### 4.1. Electrodes preparation and electrochemical characterization

The working electrodes were prepared by taking a mixture of 80wt% of Ni-MOF or Co-MOF (~4mg) with 15 wt% graphite powder and 5 wt% polytetrafluoroethylene (PTFE) binder with ethanol as a solvent. Further, the paste was packed onto the Nickel mesh (2.5 mm internal diameter and 5 mm depth). A copper wire was inserted for electrical contact. The surface was smoothed on a glossy paper and did so for each electrochemical measurement. The electrodes of different weight ratios (w/w) of graphite powder and Ni-MOF and Co-MOF were prepared and tested.

### 4.2. Cyclic voltammogram analysis of Ni-MOF and Co-MOF electrodes

Electrochemical measurements were performed on an electrochemical workstation (AUTOLAB PGSTAT302N, Switzerland) using a three-electrode cell in 0.6 M KOH electrolyte. The fabricated electrode, platinum foil and a saturated calomel electrode (SCE) served as the working electrode, counter electrode and reference electrode,

respectively. Cyclic voltammetry (CV) tests were made within the potential range of -1 to +1 V at different scan rates such as 10, 20,30,40,50, 100,150 and 200 mV Fig.5a. One of the most important parameters for practical applications is cycling stability. Fig.5b shows the stability of the Ni-MOF composite electrodes when cycled at a current 1mA for 2000 cycles. Stability of electrodes is compared in terms of losing their capacities as stability percentage. The stability of electrode calculated from following equation:

$$\text{Stability} = C_n / C_1 \times 100 \quad (1)$$

$C_n$  is the capacitance of electrode in each cycles and  $C_1$  is capacitance of electrode in the first cycle. The Ni-MOF shows an excellent retention in stability percentage of composite electrode suggesting the good stability toward long time charge-discharge applications. While the Ni-MOF electrode loses its stability fast, composite electrode maintains its stability and saves more than 90% of its capacitance of the first cycle under consecutive cycles after 2000 cycles.

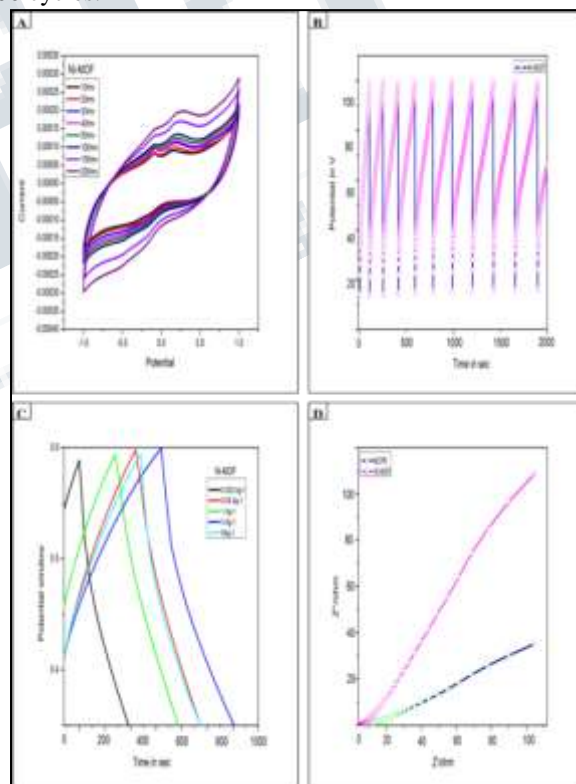


Fig.5: (a) CVs of Ni-MOF electrode in a 0.6 M KOH solution at different scan rates between 10-200 mVs<sup>-1</sup>. b) Galvanostatic Charge/ discharge curves of Ni-MOF with 2000 cycles c) Specific capacitance of Ni-MOF with different current density d) Nyquist plot of BCPE/Ni-MOF electrode in 0.6 M KOH Solution.



#### 4.2.1. Galvanostatic charge-discharge study (GCD):

Galvanostatic charge/discharge method has been used to study the capacitance characteristic of Ni-MOF electrode. Fig.5c shows the charge/discharge behaviour of Ni-MOF electrodes in the potential range from 0.0 to 0.6 V at various current densities ( $1\text{Ag}^{-1}$  to  $5\text{Ag}^{-1}$ ) to evaluate the cyclic stability and specific capacitance of Ni-MOF. As it can be seen, a triangular shape between this potential range is observed, which indicates the good columbic efficiency and ideal capacitive behaviour of Ni-MOF as electrode for application in pseudo super capacitor.

The specific capacitance was calculated using the following equation.

$$C_{sp} = It/m\Delta V \quad (2)$$

Where  $C_{sp}$  (F/g) specific capacitance,  $I$  is the constant current (A) in the charge-discharge process,  $t$  is the discharge time (sec),  $m$  is the mass of the electroactive material (g), and  $\Delta V$  (V) is the potential of Ni-MOFs. This current density was in the range  $1\text{Ag}^{-1}$  to  $5\text{Ag}^{-1}$ . We found that the specific capacitance decreases from  $202\text{ (F/g}^{-1}\text{)}$  to  $73\text{ (F/g}^{-1}\text{)}$  with increase in current density. The energy density and power density of Ni-MOF electrode are  $36.36\text{ W h kg}^{-1}$  and  $0.037\text{ W kg}^{-1}$  respectively. [23]

Electrochemical impedance spectroscopy (EIS) provides best on conducting behaviour of Ni-MOF electrodes another great tool for studying electron transfer between an electrode surface and electrolyte. Fig.5d shows the impedance graphs and matching equivalent circuits with a Ni-MOF electrode. The semicircle observed in the higher frequency region attributes to the interfacial charge transfer resistance while the straight line indicates a capacitive behaviour related to the charging mechanism at elevated frequency region. The straight line of Ni-MOF is more close to vertical line in the impedance spectra at lower frequencies, which suggests that the composites have better capacitive behaviour than Ni-MOF. Ni-MOF electrode has behaved at a frequency range from (0.01 Hz to 100 kHz) potential is 5 mV.

### 5. ELECTROCHEMICAL STUDIES OF Co-MOF.

Electrochemical studies were made to find redox behavior of Co-MOF. The electrodes were first immersed in an electrochemical cell containing 0.6 M KOH solution. The electrode performance was observed at different scan rates between 10 mV to 70 mV. The anodic peak at around -0.1 V and the cathodic peak at about -0.39 V might correspond to the conversion between different oxidation states of Co[II] to Co[III].



#### 5.1. Detection of thiocyanate ion

Fig. 6(a) shows the CVs of  $\text{SCN}^-$  solution obtained at Co-MOF electrode. The Co-MOF electrode responded quickly to the oxidation of thiocyanate at very low concentration (curve b) within the potential range 0.48 to 0.52 V. The current at anodic peak (curve c and d) has increased with an increase in  $\text{SCN}^-$  concentration. A change in the shape of the CV can be observed in presence  $\text{SCN}^-$  (curve b) at potential range between -0.3 to -0.2 V and well distinct anodic peak (curve d) appeared with increase in concentration of solution. This appearance of anodic peak is due to the formation and deposition of the reduced form of  $\text{SCN}^-$  produced during cathodic scan. This deposition might favor the oxidation process and hence the current peak of this signal (i.e., the anodic peak) rises. Further there is no alteration at cathodic peak, this might be due to the formation of dimerization of  $\text{SCN}^-$  anions to  $(\text{SCN})_2$  as shown in Fig 6 (b). These results suggest that the Co-MOF electrode has a strong affinity through surface Co-ordination for  $\text{SCN}^-$ . The possible chemical interaction of  $\text{SCN}^-$  anion is as follows.

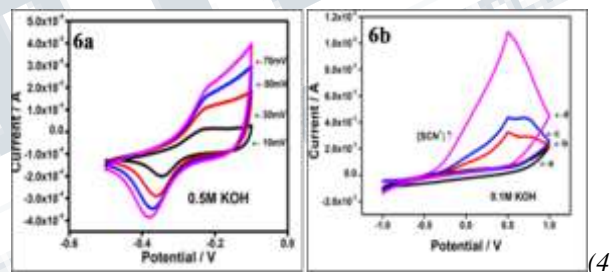
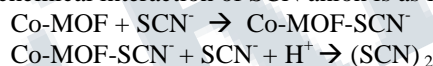


Fig. 6 (a) CVs of Co-MOF at different scan rate, (b) Cyclic voltammograms obtained by Co-MOF electrode at 50 mV/s for different concentrations of thiocyanate ion in 0.6M KOH solution (curve a) in the absence of thiocyanate ion and (curve b) in presence of thiocyanate ion.

### 6. CONCLUSION

This paper reports on the preparation of significantly active Ni-MOF material possessing high electrochemical specific capacity. As-synthesized Co-MOF are high-quality microcrystalline and porous materials. The crystal size of the hybrid MOFs prepared was found to be in the range 2 to 10  $\mu\text{m}$ . These MOFs have exhibited well-behaved redox events. Ni-MOF shows the specific capacitance up to  $202\text{ (F/g}^{-1}\text{)}$ . The specific capacitance decreases with increase in current density. These results imply about the high charge-discharge columbic efficiency, low polarization and high specific capacitance with good cycling stability in KOH media even at very low concentrations of the samples.

Hence, these Co-MOF and Ni-MOF could be harnessed as the promising materials for sensor and super capacitor applications.

### 7. REFERENCES

1. M. Ryder, J. Tan, *Mater. Sci. Technol.*, 2014, 30, 1598–1612.
2. R. R. Salunkhe, Y. Kamachi, N. L. Torad, S. M. Hwang, Z. Sun, S. X. Dou, J. H. Kim and Y. Yamauchi, *J. Mater. Chem. A*, 2014, 2, 19848–19854.
3. Y. S. Li, H. Bux, A. Feldhoff, G. L. Li, W. S. Yang and J. Caro, *Adv. Mater.*, 2010, 22, 3322–3326.
4. B. Liu, H. Shioyama, H. Jiang, X. Zhang and Q. Xu, *Carbon*, 2010, 48, 456–463.
5. R. Gruncker, V. Bon, P. Muller, U. Stoeck, S. Krause, U. Mueller, I. Senkovska and S. Kaskel, *Chem. Commun.*, 2014, 50, 3450–3452.
6. J. Yang, P. Xiong, C. Zheng, H. Qiu and M. Wei, *J. Mater. Chem. A*, 2014, 2, 16640–16644.
7. X. Xu, R. Cao, S. Jeong and J. Cho, *Nano Lett.*, 2012, 12, 4988–4991.
8. H. R. Naderi, P. Norouzi, M. R. Ganjali and H. Gholipour-Ranjbar, *Powder Technol.*, 2016, 302, 298–308.
9. R. Gruncker, V. Bon, A. Heerwig, N. Klein, P. Muller, U. Stoeck, I. A. Babur in, U. Mueller, I. Senkovska and S. Kaskel, *Chem. – Eur. J.*, 2012, 18, 13299–13303.
10. F. S. Ke, Y. S. Wu and H. Deng, *J. Solid State Chem.*, 2015, 109–121.
11. G. Krishnamurthy, B. M. Omkaramurthy, *JECSI*, 2016, ISSN-0013-466X;
12. F. Jaouen, Morozan, *Energy Environ. Sci.*, 2012, 5, 9269–9290.
13. F. Bonaccorso, L. Colombo, G. Yu, M. Stoller, V. Tozzini, A. C. Ferrari, R. S. Ruoff and V. Pellegrini, *Science*, 2015, 347, 1246501.
14. H. Ji, X. Zhao, Z. Qiao, J. Jung, Y. Zhu, Y. Lu, L. L. Zhang, A. H. MacDonald and R. S. Ruoff, *Nat. Commun.*, 2014, 5, 3317–3323.
15. N. P. Wickramaratne, J. Xu, M. Wang, L. Zhu, L. M. Dai and M. Jaroniec, *Chem. Mater.*, 2014, 26, 2820–2828.
16. Y. Jiao, Y. Liu, B. S. Yin, S. W. Zhang, F. Y. Qu and X. Wu, *Nano Energy*, 2014, 10, 90–98.
17. P. Simon and Y. Gogotsi, *Nat. Mater.*, 2008, 7, 845–854.
18. K. Naoi, *Fuel Cells*, 2010, 10, 825–833.
19. K. Naoi, W. Naoi, S. Aoyagi, J. Miyamoto and T. Kamino, *Acc. Chem. Res.*, 2013, 46, 1075–1083.
20. T. Brousse, D. Belanger and J. W. Long, *J. Electrochem. Soc.*, 2015, 162, 5185–5189.
21. V. Augustyn, P. Simon and B. Dunn, *Energy Environ. Sci.*, 2014, 7, 1597–1614.
22. F. X. Ma, L. Yu, C. Y. Xu and X. W. (David) Lou, *Energy Environ. Sci.*, 2016, 9, 862–866.
23. G. Krishnamurthy, B.M. Omkaramurthy, S. Sangeetha, *IJSEM*, 2017, ISSN 2456 -1304